# OPERATION AND PERFORMANCES OF THE LHCb EXPERIMENT*

PATRIZIA DE SIMONE

on behalf of the LHCb Collaboration

Laboratori Nazionali di Frascati, I.N.F.N.
Via E. Fermi 40, 00044 Frascati (Rome), Italy

*(Received April 29, 2011)*

The status of the LHCb experiment is presented with emphasis on the detector performance validated with the collected data. Also a particular emphasis is given to the description of the extreme running conditions that the collaboration had to handle during the first year of data taking.

DOI:10.5506/APhysPolB.42.1585
PACS numbers: 11.30.Hv, 14.40.Nd

## 1. Introduction

The LHCb detector [1] has been designed for precision studies of CP violation and rare decays of heavy flavors at the Large Hadron Collider LHC, at CERN. As the $b\bar{b}$ pairs are predominantly produced in the same forward or backward direction at high energies, the LHCb detector is a single forward arm spectrometer with a pseudo-rapidity acceptance of $1.9 < \eta < 4.9$.

The key features of the LHCb performance are:

- a flexible trigger which effectively selects particles produced in the decays of heavy mesons,
- a vertex detector with an excellent proper time resolution in order to distinguish between primary and $B$ vertices and to resolve the fast $B_s$ oscillations,
- a tracking system with a good momentum resolution in order to have a good mass resolution,
- and finally an excellent particle identification system to reduce the combinatorial background.

* Presented at the Cracow Epiphany Conference on the First Year of the LHC, Cracow, Poland, January 10–12, 2011.

The LHCb detector consist of a silicon strip Vertex Locator, the VELO, followed by a first Ring Imaging Cherenkov Counter, RICH. The tracking system made with silicon strip detectors and straw-tube drift chambers is located before and after a dipole magnet with a peak value of 1.1 Tesla. Then the second RICH detector, the calorimeter system and the muon identifier follow.

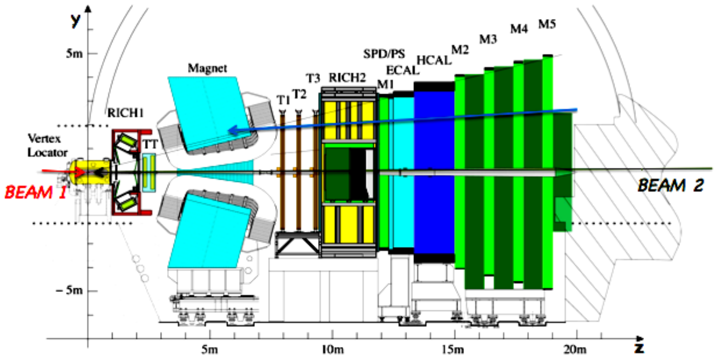


Fig. 1. Schematic view of the LHCb detector.

## 2. Running condition during 2010

The integrated luminosity at $\sqrt{s} = 7$ TeV recorded from the 30$^{\rm th}$ of March to the 29$^{\rm th}$ of October 2010 is $\sim 38$ pb$^{-1}$ with an efficiency of $\sim 90\%$. About $\frac{3}{4}$ of the data was collected during the last month when the LHC reached the peak luminosity of about $1.7\times10^{32}$ cm$^{-2}$s$^{-1}$ with 344 colliding bunches.

The optimal running conditions for LHCb require a luminosity of

$$L = \sum_{i=1}^{N_{\rm b}} \frac{f_{\rm rev} N_i^1 N_i^2 S}{4\pi\epsilon\beta^*} = 2\times10^{32}{\rm cm}^{-2}{\rm s}^{-1}\,, \tag{1}$$

where

- $N_{\rm b} = 2622$ is the number of colliding bunches per beam,
- $f_{\rm rev} = 11,245$ kHz is the bunch revolution frequency,
- $N_i^{1,2} \sim 10^{11}$ is the number of protons per bunch,
- $S \sim 673$ mrad is the beams crossing angle at LHCb,
- $\epsilon = 3.75$ $\mu$m is the normalized emittance for $E_{\rm beam} = 7$ TeV,
- $\beta^* = 10$ m is the beta function.

This choice leads to an expected average number of visible proton–proton interactions per bunch crossing in the LHCb acceptance of $\mu \sim 0.4$, simplifying the event reconstruction and reducing the radiation levels.

During the 2010 the LHC team reached a very remarkable result, about 80% of the design luminosity for LHCb, but with $\simeq$ 10% of the nominal number of colliding bunches and almost $\frac{1}{3}$ of the nominal value of $\beta^*$, leading therefore to an increase of $\mu$.

The figure 2 (left) shows the behavior of $\mu$ from July to the end of the data taking period compared to the design value. The main prompt consequences of the increase of $\mu$ are: more vertices per collision, more tracks and event complexity, an increase of the readout rate per bunch crossing, an increase of the event size and of the processing time. The LHCb collaboration appreciated very soon the importance of having a flexible trigger able to collect the data efficiently, follow the growth in luminosity, and stay within the bandwidth constraints.

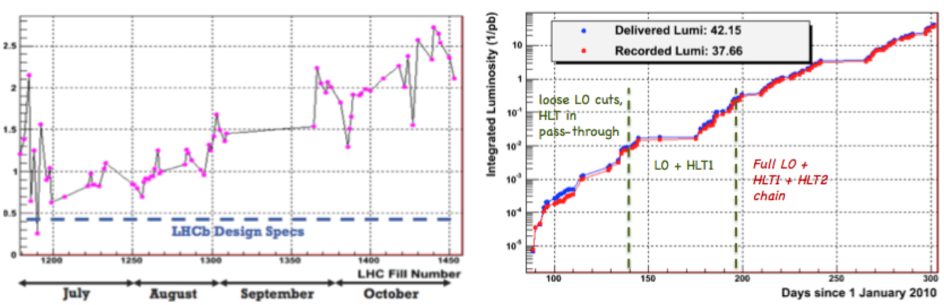


Fig. 2. The left-hand histogram shows the behavior of $\mu$ from July 2010 to the end of the data taking period compared to the design value. The right-hand histogram shows the integrated luminosity delivered (blue) and collected (red) during the 2010.

## 3. Trigger

At the LHCb design luminosity the total rate of events with reconstructible tracks in the detector acceptance is $\simeq$ 10 MHz [2], while the expected rate of interesting $B$ hadron decays is $\simeq$ 1 Hz. The main challenging requirement of the LHCb trigger system is to reduce the rate down to 2 kHz allowed by the long term data storage resources [3], while providing a good efficiency on interesting $B$ hadron decays. Two main signatures allow identifying particles from $B$ decays: high transverse momentum ($p_{\mathrm{T}}$) and non-null impact parameter, IP, with respect to the proton–proton interaction vertex. The LHCb trigger is composed of two levels, called Level 0 (L0) and High Level Trigger (HLT). The L0 hardware customized trigger uses informations from selected sub-detectors which are read-out synchronously with the LHC clock at 40 MHz: the calorimeters and the muon chambers to provide high transverse energy and/or momentum candidates, and two dedicated layers of the VELO to provide a fast estimation of the number of Primary

Vertices, PV, produced per bunch crossing. When there is an L0 positive decision starts the full readout of the detector that works at a maximum rate of 1 MHz, and the event flows into the second trigger stage, the HLT.

The HLT consists of $C^{++}$ software algorithms running on a cluster of 16000 processors named the Event Filter Farm (EFF), and it has access to the full event information. However, a complete reconstruction is not feasible at 1 MHz, this is why the HLT algorithm [4] is divided into two sequential phases called HLT1 and HLT2:

- **HLT1** applies a partial reconstruction of the events, which are first classified according to their L0 origin (leptons, $\gamma$s, hadron candidates) entering then into different sequences of algorithms that will confirm or reject the L0 decision. HLT1 selects a maximum event rate of 30 kHz.
- **HLT2** starts with the full reconstruction of the events that is similar to the one that will be applied offline. Inclusive selections searching for generic signatures (displaced vertices, dilepton pairs, *etc.*) as well as exclusive fully reconstructed $B$ decays are tried.

The selected events are finally sent to the storage with a maximum rate of 2 kHz and an average size of $\sim$ 35 kB.

The plot in figure 2 (right) reports the delivered and the recorded integrated luminosity during the year 2010, and it is divided in three main periods:

1. The LHC initial low collision rate was easily absorbed with a trigger configuration based on the same activity being found in the calorimeter and/or in the muon systems, *L0 minimum bias trigger*, and the HLT selections run in *pass through* mode, so that their performances could be monitored.
2. The increase of luminosity during the second period (Spring 2010) necessitated the deployment of the L0 *high* $p_{\mathrm{T}}$ trigger, and the introduction of the HLT1 in soft rejection mode. It was possible, however, to set the hight $p_{\mathrm{T}}$ thresholds to lower than nominal values so that the efficiencies on hadronic decays of prompt $D$ hadrons are about 4 times higher with respect to the nominal settings optimized for the $B$ hadrons decays.
3. Starting from July 2010 the trigger configurations were rapidly evolving to accommodate not only the increasing of the luminosity but also the number of visible interactions per bunch crossing, $\mu$. During this period the thresholds of the L0 were increased in order to maintain the input rate to the HLT farm around 300 kHz. To reduce the processing time some global event cuts have been introduced: multiplicity in the scintillator layer in front of the calorimeters SPD and number of hits

in the VELO. Essentially, the main aim of these actions was to avoid to reach the bandwidth limitations, it must be considered that for $\mu \simeq 2.5$ the event size becomes about 65 kB. In addition, in September 400 nodes have been added in less then three days in order to double the EFF capacity.

## 4. The tracking system

The vertex detector, VELO, is composed of 21 silicon microstrip stations perpendicular to the beam direction, with a $R$–$\Phi$ geometry and a strip pitch between 40 and 100 $\mu$m. The sensors are placed at a radial distance of 7 mm from the beams, which is smaller than the aperture required by LHC during the injection and the machine developments. This explains why the VELO consists of two equal halves that can be retracted at a distance of 30 mm from the beam during the injection and inserted back when stable beams are declared: the closing/opening procedure takes few minutes. The sensors' alignment is known to better than few $\mu$ms. The individual hit resolution of the sensors is a strong function of the sensor pitch and the projected angle as shown in figure 3. A single hit resolution of 4 $\mu$m has been achieved at optimal projected angle for the smallest pitch size.

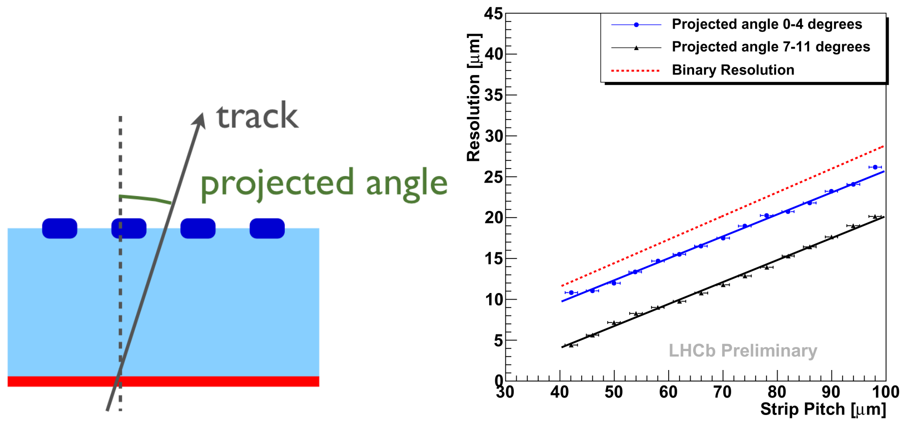


Fig. 3. The left picture shows a sketch of the projected angle. The right-hand histogram shows the VELO hit resolution *versus* the strip pitch in two projected angle regions.

Assuming that all tracks originate from the primary interaction, the resolution on the impact parameter can be determined as the spread of its distribution. The figure 4 (left) shows the resolution of the $X$ component of IP as a function of the inverse of the transverse momentum. The primary vertex resolution is strongly correlated to the number of tracks that make the vertex. The PV resolution is measured by randomly splitting the track sample of each event into two sets and comparing two vertices with the same number of tracks, see figure 4 (right). The method has been validated with the MC. For a vertex with 25 tracks the resolution has been found to be 16 $\mu$m in $X$ and $Y$, and 76 $\mu$m in $Z$.

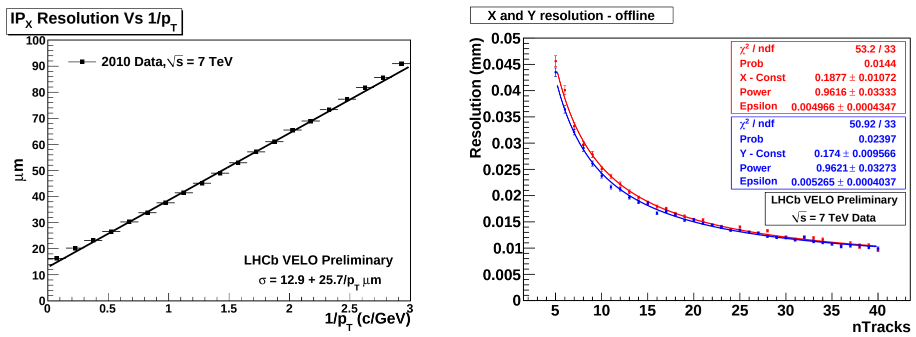


Fig. 4. The left-hand histogram shows the IP$_X$ resolution as a function of $1/p_{\mathrm{T}}$. The right-hand histogram shows the PV$_X$ (red) and PV$_Y$ (blue) resolutions as a function of the track multiplicity.

The silicon trackers of the tracking system are composed of the Tracker Turicensis TT upstream of the magnet and of the Inner Tracker IT downstream of the magnet.

The TT is composed of 2 stations with 4 layers of silicon microstrip sensors with a pitch of 183 $\mu$m that cover the full acceptance of the LHCb detector. The two central layers of each station are rotated by a stereo angle of $\pm 5°$.

Each of the three stations of the Inner Tracker consist of 4 individual boxes arranged around the beam pipe: each box contains 4 layers of silicon microstrips with a strip pitch of 198 $\mu$m. Also the two central layers of each box are rotated by a stereo angle of $\pm 5°$.

The single hit resolution is evaluated by the unbiased residual (hit-track) distribution. The resolution for both detectors are comparable $\simeq 55$ $\mu$m, and in good agreement with the MC expectations considering that the current alignment accuracy is $\simeq 35$ $\mu$m for the TT and $\simeq 16$ $\mu$m for the IT.

The Outer Tracker OT surrounds the IT detector to complete the acceptance of the LHCb. It is composed of three stations each with 4 double layers of straw-tubes drift chambers with a diameter of $\sim 4.9$ mm. The gas mixture is composed of argon (70%), $CO_2$(28.5%), and $O_2$(1.5%). As for the other tracking detectors, the two central layers of each station are tilted by $\pm 5°$ respect to the vertical direction ($Y$). The hit resolution is obtained from the residual of the space-time relations and is $\simeq 250$ $\mu$m in very good agreement with the MC expectation.

An excellent momentum resolution is essential to obtain a good invariant mass resolution, in particular for two bodies decays, which leads to higher sensitivity in rare decays searches as well as to lower the background levels in general. In LHCb, a very good mass resolution is obtained, for example we measure a resolution of 3.3 MeV$/c^2$ for $K_S \to \pi^+\pi^-$, and $\simeq 25$ MeV$/c^2$ for $B \to K\pi$, see figure 5. The mass resolutions are in general in very good agreement with the MC expectations.

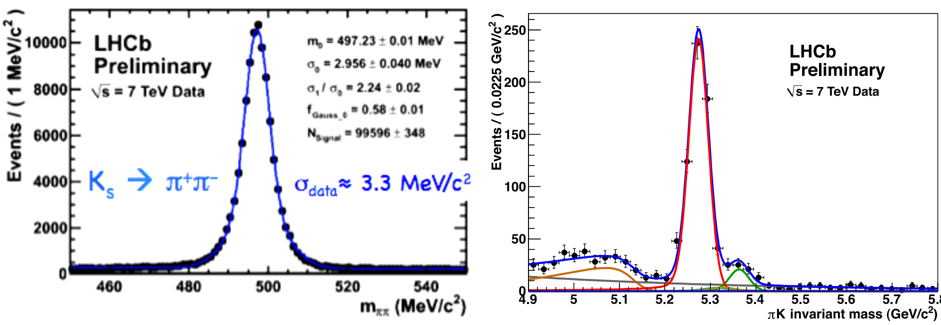


Fig. 5. The left-hand histogram shows the mass invariant for $K_S \to \pi\pi$, while the right-hand histogram shows the mass invariant for $B \to K\pi$ ($\sigma \simeq 25$ MeV$/c^2$).

The reconstruction of high tracks multiplicity of beauty and charm decay vertices require a high tracking efficiency. Several methods have been developed to measure the efficiency from the data. One based on the *tag and probe* method uses the $K_S \to \pi\pi$: the *tag* pion is completely reconstructed by the tracking system while the *probe* one is reconstructed using only the VELO segment matched with a cluster in the calorimeter, see figure 6 (left). The measured efficiency as a function of the transverse momentum in shown in figure 6 (right), it is about 95% for tracks with $p_T > 100$ MeV$/c$ which covers the full physics range of the experiment.

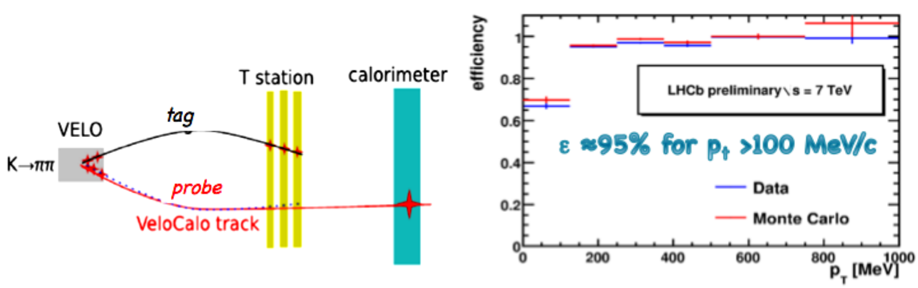


Fig. 6. The left-hand picture is a sketch to describe the *tag and probe* method with $K_S \to \pi\pi$ decays. The right-hand histogram shows the tracking efficiency as a function of $p_T$ for data (blue) and Monte Carlo (red).

## 5. The RICH detectors

Pion, kaon and proton identification is based on using the information from two RICH detectors. The upstream detector RICH1 covers low momentum range from 1 GeV/$c$ to about 70 GeV/$c$ using aereogel and $C_4F_{10}$ radiators, while the downstream detector RICH2 covers high momentum range from $\simeq$ 15 GeV/$c$ up to and beyond 100 GeV/$c$ using a $CF_4$ radiator. RICH1 covers the full acceptance, while RICH2 located downstream the magnet has a limited angular acceptance but covers the region where high momentum particle are produced. In both RICH detectors the focusing of the Cherenkov light is done using a combinations of spherical and flat mirrors to reflect the images out of the detector acceptance. Hybrid Photon Detectors HPD are used to detect the Cherenkov $\gamma$s ($\lambda$ = 200–600 nm).

Figure 7 (left) shows the hit pixels in the RICH photodetectors. Rings are superimposed corresponding to the different particle hypotheses. The agreement of the hits with the kaon hypothesis for the selected ring is evident.

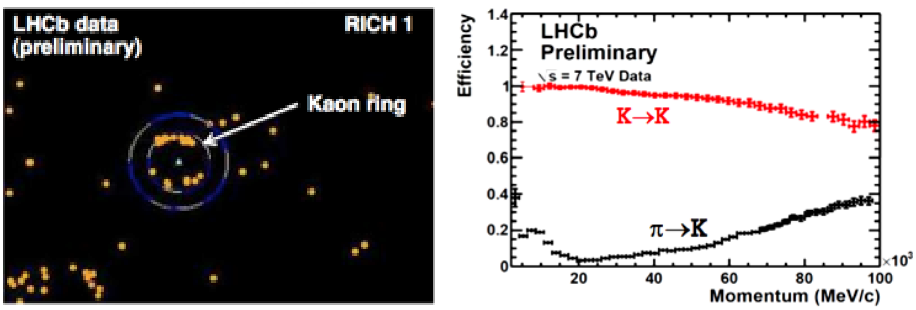


Fig. 7. The left-hand picture shows the Cherenkov light: the (orange) points. The right-hand histogram shows the RICH $K/\pi$ separation performance as a function of the momentum.

The performance of pion and proton identification has been studied using the decay products of the reconstructed $K_S$ mesons and $\Lambda$ baryons. For the kaon identification, reconstructed $\phi \to K^+K^-$ decays have been used. The plot in figure 7 (right) shows the $K/\pi$ separation performance currently achieved.

## 6. Calorimeters

The LHCb calorimeter system selects the transverse energy of hadron, electron and photon candidates for the first level trigger L0. It provides also the identification of these particles as well as the measurement of their energies and positions. A classical structure of an electromagnetic calorimeter

ECAL followed by an hadron calorimeter HCAL has been adopted. The shashlik technology has been chosen for the ECAL: 66 layers of 2 mm Pb and 4 mm scintillator, 25 $X_0$, the light is collected by Wave Length Shifter WLS fibers. The HCAL is a sandwich of iron and scintillator tiles (5.6 $\lambda_i$).

To determine the nature, charged or neutral, of the energy deposited at the L0 trigger level, before the ECAL there is a 2.5 $X_0$ lead converter sandwiched between two scintillator planes 15 mm thick (Preshower PS and Scintillator Pad Detector SPD). Also here the light is collected with WLS fibers.

The time alignment of the calorimeter system is at $\simeq$ 1 ns level. The ECAL energy resolution is $\sigma/E \simeq \frac{9\%}{\sqrt{E}} \oplus 0.8\%$, and the HCAL energy resolution is $\sigma/E \simeq \frac{69\%}{\sqrt{E}} \oplus 9\%$. Electron and photon identification is mainly based on the balance of the energy deposited in the calorimeter system and the track momentum, and the matching between the corrected barycenter position of the calorimeter cluster and the extrapolated track impact point. The electromagnetic calorimeter has been calibrated to $\sim$ 2% accuracy resulting in a $\pi^0$ invariant mass resolution of $\sim$ 7 MeV/$c$ as shown in figure 8 (right).

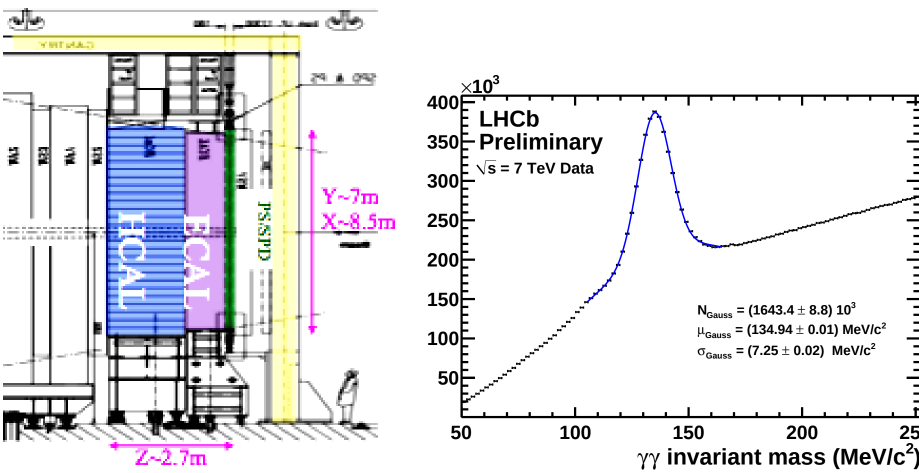


Fig. 8. The left-hand picture shows a sketch of the LHCb calorimeter system. The right-hand histogram shows the invariant mass of two $\gamma$s reconstructed in the electromagnetic calorimeter.

The histograms in figure 9 show examples of electrons and $\gamma$s identification with the LHCb calorimeter system.

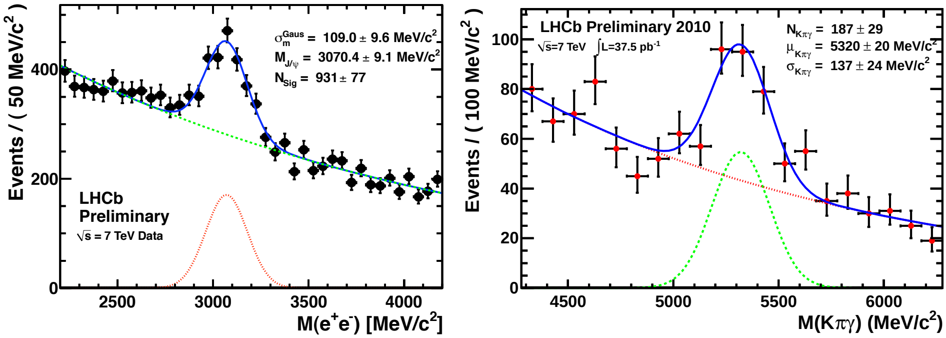


Fig. 9. The left-hand histogram shows the $J/\psi$ invariant mass from the $e^+e^-$ decay channel. The right-hand histogram shows the invariant mass of the $B$ meson from the radiative decay to $\gamma K^*$.

## 7. Muon system

The LHCb muon system selects muon candidates with high transverse momentum for the first level trigger L0, and provides the identification of these particles. The muon system is composed of 5 stations (M1–M5) of rectangular shape, placed along the beam axis. Stations M2 to M5 are placed downstream the calorimeters and are sandwiched with iron filters 80 cm thick to select penetrating muons. The minimum momentum of a muon to cross the system is $\sim 6$ GeV/$c$ since the total absorber thickness, including the calorimeters, is $\sim 20\ \lambda_i$. Station M1 is placed before the calorimeters to improve the transverse momentum evaluation at the level of the L0 trigger. All the stations are instrumented with 2 double gaps of Multiwires Proportional Chambers MWPC, except the highest rate region of the M1 station (the inner area closest to the beam line) that is instrumented with triple GEM chambers. The gas mixture is Ar (40%), $CO_2$ (55%), $CF_4$ (5%) for the MWPC, and Ar (45%), $CO_2$ (15%), $CF_4$ (40%) for the triple GEM. The detector provides space point measurements of the incident tracks, and the readout is done with logical pads with a projective geometry. The efficiency of the muon stations during the 2010 data taking period has been monitored: it was stable and bigger than 99% as expected.

The muons are identified by extrapolating well reconstructed tracks with $P \geq 3$ GeV/$c$ into the muon stations and matching the tracks with hits within the corresponding field of interest. Using a sample of reconstructed $J/\psi \to \mu^+\mu^-$ decays, the muon identification efficiency has been measured to be $(97.3 \pm 1.2)\%$ which is in good agreement with the Monte Carlo expectation, see figure 10. The corresponding $\mu/\pi$ and $\mu/K$ misidentification rates are dominated by the $\pi$ and $K$ decays in flight and measured to be

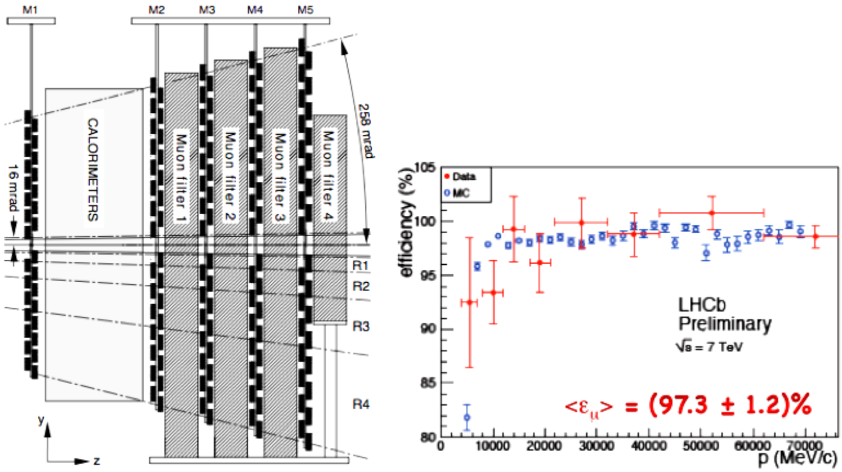


Fig. 10. The left-hand picture shows a sketch of the LHCb muon system. The right-hand histogram shows the muon identification efficiency as a function of the muon momentum.

below 1% for $P > 20$ GeV/$c$, using large samples of $K_S \to \pi\pi$, $\phi \to KK$ and $\Lambda \to p\pi$ decays. The histograms in figure 11 show examples of muon identification with the LHCb muon system.

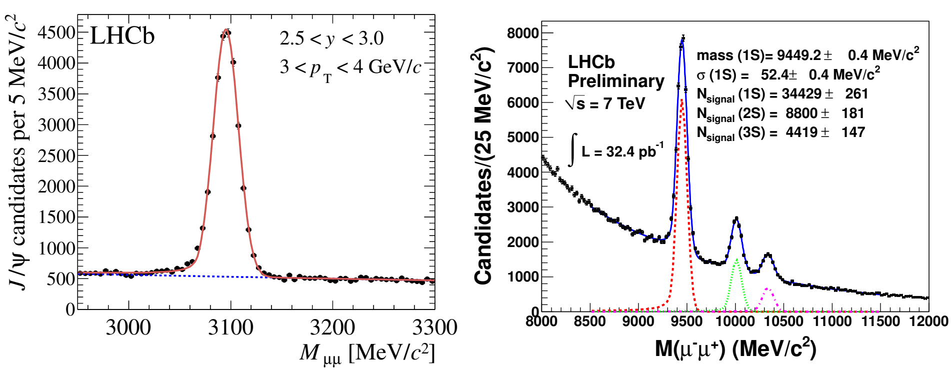


Fig. 11. The left-hand histogram shows the $J/\psi$ invariant mass from the $\mu^+\mu^-$ decay channel [5]. The right-hand histogram shows the invariant masses of the $\Upsilon$ resonances, $\Upsilon(1S)$, $\Upsilon(2S)$ and $\Upsilon(3S)$ from left to right. The superimposed curves on the signal and the yields are the result of a fit described in [6].

## 8. Conclusions

The performance of the LHCb detector during the 2010 was excellent, and the challenges of this first year of running in extreme conditions have been overcome, allowing the data-taking to follow efficiently the growth in luminosity.

The accumulated data sample of $\sim 38$ pb$^{-1}$ gave us the possibility to produce the first important physics results which have been presented at this conference [7, 8, 9, 10, 11], and recently the LHCb collaboration presented 14 talks at the Beauty Conference 2011.

In March started the new physics run 2011/2012 at the center of mass energy of 7 TeV with the aim to collect a data sample of about 2 fb$^{-1}$. The foreseen maximum instantaneous luminosity at the LHCb interaction region is $\simeq 3 \times 10^{32}$ cm$^{-2}$s$^{-1}$. To face safely this new years of running, new 400 nodes have been added to the EFF during the winter shutdown. Also a big effort have been done to improve the timing of the HLT algorithms, mainly the timing of the track fit procedure ($\sim 45\%$ improvement), keeping equal trigger efficiency performance.

## REFERENCES

[1] [LHCb Collaboration] A.A. Alves *et al.*, *JINST* **3**, S08005 (2008).

[2] [LHCb Collaboration], LHCb Trigger System Technical Design Report, CERN-LHCC-2003-31, 2003.

[3] [LHCb Collaboration], LHCb Computing Technical Design Report, CERN-LHCC-2005-19, 2005.

[4] [LHCb Collaboration] J. Albrecht *et al.*, *Nucl. Phys. B Proc. Suppl.* **187**, 237 (2009).

[5] [LHCb Collaboration] R. Aaij *et al.*, *Eur. Phys. J.* **C71**, 1645 (2011).

[6] [LHCb Collaboration], Measurement of the $\Upsilon(1S)$ Production Cross-section at $\sqrt{s} = 7$ TeV in LHCb, LHCb-CONF-2011-016, April 20, 2011.

[7] E. Santovetti, *Acta Phys. Pol. B* **42**, 1567 (2011), this issue.

[8] R. Oldeman, *Acta Phys. Pol. B* **42**, 1539 (2011), this issue.

[9] R. Aaij, *Acta Phys. Pol. B* **42**, 1353 (2011), this issue.

[10] K. Mueller, *Acta Phys. Pol. B* **42**, 1531 (2011), this issue.

[11] B. Popovici, *Acta Phys. Pol. B* **42**, 1547 (2011), this issue.